



Article

Low-Symmetry Mixed Fluorinated Subphthalocyanines as Fluorescence Imaging Probes in MDA-MB-231 Breast Tumor Cells

Katherine J. McAuliffe, Megan A. Kaster, Regina G. Szlag and Evan R. Trivedi *

Department of Chemistry, Oakland University, Rochester, MI 48309, USA; kjmcauliffe@oakland.edu (K.J.M.); makaster@oakland.edu (M.A.K.); rgszlag@oakland.edu (R.G.S.)

* Correspondence: trivedi@oakland.edu; Tel.: +1-248-370-2147

Academic Editor: Nick Hadjiliadis

Received: 12 May 2017; Accepted: 30 May 2017; Published: 1 June 2017

Abstract: Boron subphthalocyanines (SPcs) are aromatic macrocycles that possess a combination of physical and optical properties that make them excellent candidates for application as fluorescent imaging probes. These molecules have intense electronic absorption and emission, and structural versatility that allows for specific tuning of physical properties. Herein, we report the synthesis of a series of low-symmetry fluorinated SPcs and compare them to analogous compounds with varying numbers of peripheral fluorine atoms and varied aromaticity. Across the series, with increasing addition of fluorine atoms to the periphery of the ring, a downfield chemical shift in ^{19}F NMR and a bathochromic shift of electronic absorption were observed. Expanding the size of the aromatic ring by replacing peripheral benzo- groups with naphtho- groups prompted a far more drastic bathochromic shift to absorption and emission. Fluorescence quantum yields (Φ_f) proved to be sufficiently high to observe intracellular fluorescence from MDA-MB-231 breast tumor cells in vitro by epifluorescence microscopy; fluorination proved vital for this purpose to improve solubility. This report lays the groundwork for the future development of these promising SPcs for their ultimate application as near-infrared (NIR) fluorescent imaging probes in biological systems.

Keywords: subphthalocyanine; fluorescence imaging; ^{19}F NMR; fluorescence microscopy

1. Introduction

Boron subphthalocyanines (SPcs) are 14π -electron tripyrrolic macrocycles that were first discovered in 1972 [1], and have garnered significant attention for their structural versatility and optical properties, which has recently been reviewed extensively [2,3]. The ring system is conical in shape with an apical central boron with an axial ligand, usually a halogen ($X = \text{F}, \text{Cl}, \text{Br}$) [4], making these macrocycles more polar and less aggregative than their planar tetrapyrrole phthalocyanine (Pc) cousins. Like Pcs, SPcs are synthesized by the templated cyclization of phthalonitrile derivatives. Synthesis from a C_{2v} symmetric phthalonitrile yields C_{3v} symmetric SPcs, whereas lower symmetry phthalonitrile starting materials yield a mixture of constitutional isomers (C_1 and C_3) that are axially chiral [5]. Low-symmetry elements can also be introduced through a mixed cyclization with multiple phthalonitrile derivatives; co-cyclization of phthalonitrile with naphthalene-2,3-dicarbonitrile, for example, yields a series of four macrocycles denoted $A_{3-n}B_n(\text{SPc})$ where "A" is a peripheral benzo moiety and "B" is a peripheral naphthalene [6]. Similar strategies have been employed to produce fluorinated A_2B and AB_2 type SPcs [7], designer pyrene fused SPcs [8], and even core-expanded analogues with annulated 6- and 7-membered rings [9]. We are particularly interested in using a cross-cyclization approach to synthetically tune SPc properties for application as fluorescent tumor cell imaging probes.

Fluorescence imaging with a contrast agent is a growing technique for the study and diagnosis of cancer [10–12]. A fluorescence probe that absorbs and emits in the near-infrared (NIR) is particularly valuable due to the ability for NIR light to effectively penetrate soft tissue [13]. One promising application of this technology is in the real-time intraoperative detection of cancer in humans [14,15], a prospect that would greatly aid surgical oncologists. Development of new contrast agents with optimal photophysical properties and some sort of preferential tumor accumulation is, therefore, imperative.

Pyrrolic macrocycles have intense absorption and fluorescence [16], warranting their application as biomedical fluorescence imaging agents. Selected Pc derivatives have seen success on this front [17–20]; far fewer examples of SPc fluorescence within cells exist in the literature [21,22]. In each SPc case, the axial ligand of boron is exchanged to improve solubility. Herein, we describe a series of mixed SPcs and slightly larger subnaphthalocyanines (SNcs) with a variable number of peripheral fluorine atoms ($\# F = 0, 4, 8, \text{ or } 12$). Fluorine was chosen here for its ability to bathochromically shift photophysical properties toward the NIR [23,24], the pharmacological inertness of the C–F bond in drug design [25], and the effects that a variable number of fluorines will have on lipophilicity and biodistribution within the cell [26]. Relevant photophysical properties have been tabulated and preliminary studies of intracellular fluorescence is reported.

2. Results and Discussion

2.1. Synthesis of SPcs

Two types of macrocycles have been synthesized with variable peripheral groups of the form $\text{SPc}(A_nB_{3-n})$ and $\text{SPc}(A_nC_{3-n})$, where “A” is tetrafluorobenzo-, “B” is benzo-, “C” is naphtho-, and n is an integer 0–3 (Figure 1). A modified literature procedure was employed, whereby aromatic dinitriles were heated to 140 °C in *p*-xylene with an excess (1.5 equivalents) of BCl_3 . The previously reported compounds $\text{SPc}(A_3)$ [27], $\text{SPc}(B_3)$ [1], and $\text{SPc}(C_3)$ [6], can be prepared from the lone cyclization of tetrafluorophthalonitrile, phthalonitrile, and naphthalene-2,3-dicarbonitrile, respectively; mixed “AB” and “AC” SPcs were prepared by co-cyclizing dinitriles with varying stoichiometry. While the “AC” series of SPcs have been previously reported [7], $\text{SPc}(A_2B)$ and $\text{SPc}(AB_2)$ are novel so their synthesis will be discussed in more detail.

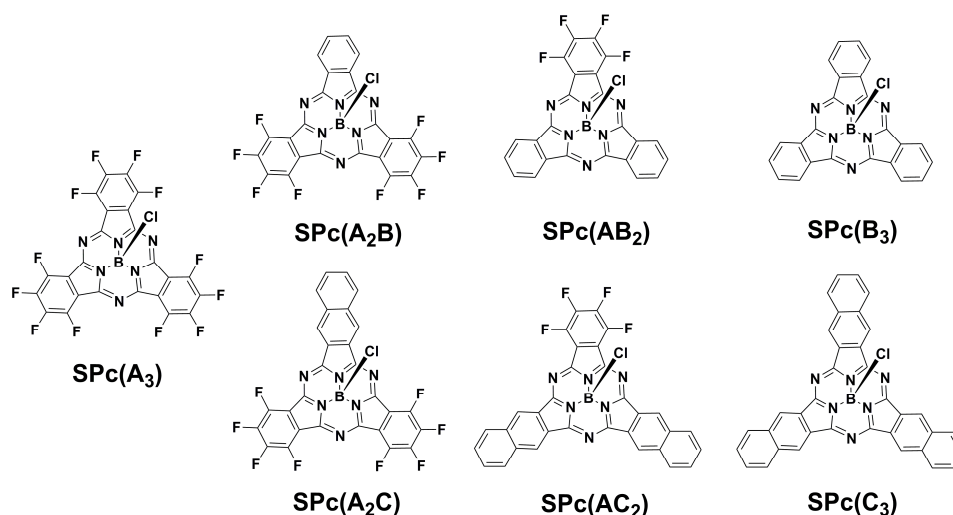


Figure 1. Mixed fluorinated boron subphthalocyanines (SPcs).

Co-cyclization with equimolar amounts of tetrafluorophthalonitrile and phthalonitrile yields all four $\text{SPc}(A_nB_{n-3})$. In order to optimize yields, separate reactions were completed using a 3:1 stoichiometric ratio of one cyclization partner to the other. An excess of phthalonitrile yielded

SPc(AB₂) in *ca.* 10% yield, whereas an excess of tetrafluorophthalonitrile yielded SPc(A₂B) at *ca.* 30%. We attribute the disparity in yield to the relative cyclization rates of the two starting materials. In sub-stoichiometric co-cyclization reactions, SPc(A₃) was observed by TLC but not collected. Purification by flash chromatography of the SPc mixtures was achieved and identity and purity were confirmed by HRMS, NMR (¹⁹F, ¹H), and analytical HPLC (Figures S1–S8).

2.2. ¹⁹F NMR Characterization of SPcs

One convenient benefit of fluorinated SPcs with varying symmetries is that each would be expected to have a signature ¹⁹F NMR profile. Each SPc contains two types of fluorine atoms, α-F (non-peripheral) and β-F (peripheral), relative to the central pyrroles. Based on ¹⁹F NMR trends observed for various substituted fluorobenzenes [28], and analogous ¹H NMR data for SPcs [2], we assign the non-peripheral F-atoms to be further upfield (more negative ppm) than peripheral F-atoms (Table 1). As expected, the C_{3v} SPc(A₃) and two C_s SPc(AX₂) exhibited two signals that appeared as doublets with J_{FF}~17 Hz. The expected meta-coupling was not resolved. The two C_s SPc(A₂X) compounds exhibited four signals, two in the α-F region and two in the β-F region, as complex multiplets. The general trend across the series is that the fluorine atoms provide a deshielding effect, with the signal from the most fluorinated SPc appearing the furthest downfield (δ –136.7). The naphtho- functionalized “AC” SPcs are more shielded than the analogous benzo- “AB” SPcs with the furthest upfield signal being for SPc(AC₂). These data not only confirm identity of the fluorinated SPcs studied here, but also provide a library of ¹⁹F chemical shifts for SPcs to be used in future synthetic refinement.

Table 1. ¹⁹F NMR data for fluorinated SPcs ¹.

Compound	α-F-δ (ppm)	β-F-δ (ppm)
SPc(A ₃)	–147.4 (d) ²	–136.7 (d)
SPc(A ₂ B)	–149.2 (m), –149.9 (m)	–138.5 (m), –138.8 (m)
SPc(AB ₂)	–151.7 (d)	–140.3 (d)
SPc(A ₂ C)	–149.2 (m), –150.6 (m)	–138.8 (m), –138.9 (m)
SPc(AC ₂)	–153.7 (d)	–141.8 (d)

¹ Samples in CDCl₃ at 376.5 MHz. ² multiplicity.

2.3. Photophysical Properties of SPcs

Much like the more common porphyrins and Pcs, SPcs possess two major absorptions [29]: the Soret-band in the UV region (~300–400 nm) and the Q-band in the visible (>500 nm). The Q-band is sensitive to both peripheral functionalization and symmetry of the macrocycle. Peripheral functionalization has potential to bathochromically shift absorption toward the NIR and symmetry has effects on the shape of the spectrum; low-symmetry macrocycles show splitting of the Q-band due to lower degeneracy of the lowest unoccupied molecular orbital (LUMO). Indeed, the perfectly symmetrical (C_{3v}) SPcs (SPc(A₃), SPc(B₃), and SPc(C₃)) exhibited a single peak in the Q-band region, whereas low-symmetry (C_s) SPcs (SPc(A₂B), SPc(AB₂), SPc(A₂C), and SPc(AC₂)) showed more complex splitting of the Q-band (Figure 2). Fluorescence (λ_f) occurs slightly red-shifted from the Q-band absorption (λ_{max}), the difference in energy between the two being termed the Stokes shift. The efficiency of fluorescence can be quantified by the quantum yield of fluorescence (Φ_f). Each of these parameters are summarized in Table 2 in tetrahydrofuran (THF) solution.

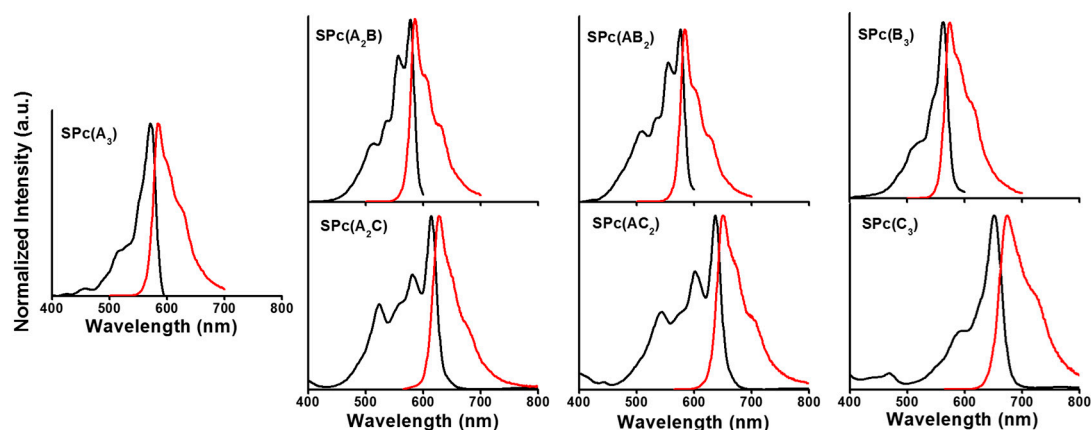


Figure 2. Electronic absorption (black) and emission (red) spectra for mixed fluorinated SPcs.

For the “AB” series of SPcs, the shifting of peak positions was dominated by the addition of fluorine. The electron withdrawing groups stabilize the LUMO, thereby red-shifting the emission as far as ca. 585 nm. For the “AC” series, the effect of adding additional fused benzo rings was far greater than that of peripheral fluorine. Each successive addition of a fused benzo ring red-shifted the emission by over 20 nm, despite the deletion of electron withdrawing fluorine atoms. This side by side comparison of “AB” and “AC” SPcs demonstrates the synthetic tunability of optical properties, with two members of the series (SPc(AC₂) and SPc(C₃)) approaching the edge of the NIR window of maximum light penetration. Quantum yields were nearly consistent across the series, within the error of the measurement, with a few outliers on the low-end. Quantum yields will be discussed in more detail below with respect to *in vitro* cell imaging studies below.

Table 2. Summary of SPc photophysical parameters ¹.

Compound	Absorption (λ_{max} , nm)	Emission (λ_f , nm)	Stokes Shift (cm^{-1})	Quantum Yield (Φ_f)
SPc(A ₃)	571	584	390	0.30
SPc(A ₂ B)	578	585	210	0.19
SPc(AB ₂)	572	578	180	0.26
SPc(B ₃)	563	574	460	0.29
SPc(A ₂ C)	613	628	390	0.21
SPc(AC ₂)	637	650	310	0.16
SPc(C ₃)	651	674	520	0.28

¹ Samples in THF.

2.4. *In Vitro* Epifluorescence Microscopy in MDA-MB-231 Breast Tumor Cells

While the majority of compounds discussed here are unsuitable for ultimate application in the NIR region, proof of concept experiments were conducted by epifluorescence microscopy to judge how synthetic modifications may influence cellular uptake and/or biodistribution. The “AC” series of compounds, while their optical properties are closer to ideal, proved insufficiently soluble in aqueous cell culture medium for testing. The “AB” series of SPcs made stable solutions in media with the addition of 0.2% dimethylsulfoxide (DMSO) as a solubilizing agent. Compounds such as these, at the edge of the usable solubility range, have greater potential to interact with hydrophobic proteins and membranes within the cell, which can positively effect biodistribution and uptake.

The MDA-MB-231 breast tumor cells were plated and allowed to grow to 50% confluency before being treated with SPc solutions (50 μ M) for 15 min (Figure 3). Brightfield and epifluorescence micrographs were collected on the live cells using an orange TRITC filter set. Fluorinated SPcs all showed strong intracellular fluorescence relative to DMSO treated control cells, whereas the signal from SPc(B₃) was far weaker, albeit present. Two factors dictate the brightness of cell images: (1) the extent of cellular uptake and (2) the quantum yield of the probe. Considering that the quantum yields of

these SPc are within the same order of magnitude, one can assume that the cellular uptake of SPc(B₃) is far less than the others under the same conditions. This observation is not particularly surprising since the SPc(B₃) is devoid of solubilizing fluorine atoms. The key observation here that will guide future synthetic refinement is that simple addition of fluorine atoms to the periphery of the SPc can drastically change biocompatibility.

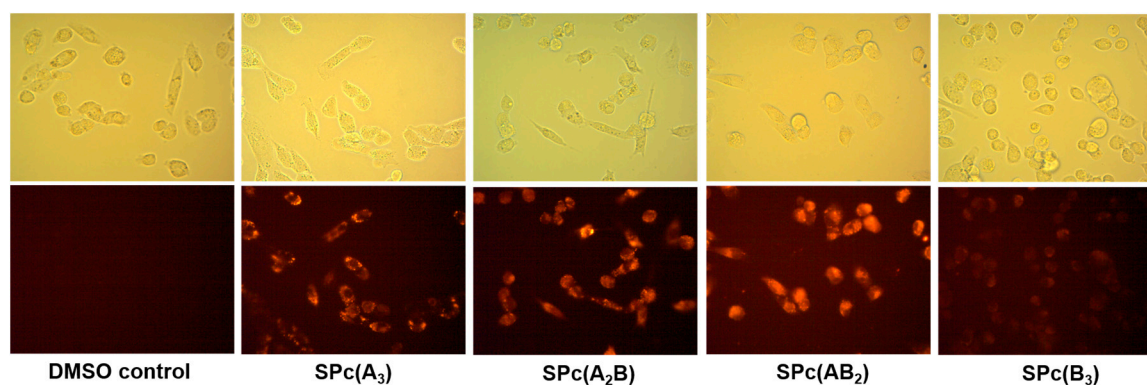


Figure 3. Brightfield (**upper**) and epifluorescence (**lower**) $\lambda_{\text{ex}} = \text{BP } 528\text{--}553 \text{ nm}$, $\lambda_{\text{em}} = \text{BP } 578\text{--}633 \text{ nm}$) of MDA-MB-231 breast tumor cells treated with $50 \mu\text{M}$ SPc for 15 min ($400\times$).

3. Materials and Methods

3.1. Materials

Reagents and chemicals, including silica gel (60 Å, 230–400 mesh), were purchased from VWR International (Radnor, PA, USA) and used without further purification unless otherwise noted. Tetrafluorophthalonitrile (TFPN) was purchased from TCI America (Portland, OR, USA) and boron subphthalocyanine chloride (SPc(B₃)) and boron subnaphthalocyanine chloride (SPc(C₃)) were purchased from Sigma-Aldrich (St. Louis, MO, USA).

3.2. General Considerations

Nuclear magnetic resonance (NMR) spectra were recorded on an Avance III (400 MHz, Bruker) spectrophotometer. ¹⁹F NMR spectra were recorded using trifluoroacetic acid as a standard ($\delta = -76.55 \text{ ppm}$). Mass spectrometry was performed on an LC/MS 6545 Q-TOF (Agilent, Santa Clara, CA, USA) in APCI mode. Purity analysis by HPLC was performed on an Agilent 1100 system with diode array detector and C8 ZORBAX Eclipse Plus column (Agilent). Absorption data was collected on a Cary-100 UV-Vis spectrophotometer (Agilent) in double-beam mode using 1 cm path quartz cuvettes. Corrected fluorescence spectra were collected on a Fluorolog 3 fluorometer (Horiba Jobin-Yvon, Edison, NJ, USA) equipped with an R928 PMT (Hamamatsu, Shizuoka, Japan). Solutions were prepared such that absorption remained below 0.1 AU to prevent reabsorption and self-quenching. Fluorescence spectra were recording using an excitation wavelength corresponding to the maximum Q-band absorption.

3.3. Synthesis

Naphthalene-2,3-dicarbonitrile [30], boron 1,2,3,4,8,9,10,11,15,16,17,18-dodecafluorosubphthalocyanine chloride (SPc(A₃)) [27], boron 1,2,3,4,8,9,10,11-octafluoro-naphtho[*b*] subphthalocyanine chloride (SPc(A₂C)), boron 1,2,3,4-tetrafluoro-dinaphtho[*b,g*] subphthalocyanine chloride (SPc(AC₂)) were prepared by literature procedure [7]. Hitherto unreported characterization data (¹⁹F NMR) are summarized for SPc(A₃), SPc(A₂C), and SPc(AC₂).

SPc(A₂B)—*Boron 1,2,3,4,8,9,10,11-octafluorophthalocyanine chloride*. To a 25 mL roundbottom flask was added phthalonitrile (0.091 g, 0.71 mmol) and tetrafluorophthalonitrile (0.422 g, 2.11 mmol). The flask was purged with N₂, *p*-xylene (8 mL) was added, and the flask was heated to 140 °C. A solution of BCl₃ (1 M in *p*-xylene, 1.05 mL, 1.05 mmol) was added, resulting in a yellow solution. After approximately five minutes, the solution changed color to dark red. The reaction was stirred for 40 min, after which the solvent was reduced in vacuo. The resulting dark purple solid was dissolved in dichloromethane and filtered through a plug of silica gel. The resulting sample was purified by flash chromatography on silica gel (1:9 ethyl acetate: hexane). A dark purple solid was obtained (0.129 g, 32%). ¹H NMR (400 MHz, CDCl₃) δ (ppm): 8.06 (dd, *J* = 6 Hz, 3 Hz, 2H), 8.94 (dd, *J* = 6 Hz, 3 Hz, 2H); ¹⁹F NMR (376 MHz, CDCl₃) δ (ppm): −138.5 (m, 2F), −138.8 (m, 2F), −149.2 (m, 2F), −149.9 (m, 2F); HR-LCMS APCI: calcd. for (C₂₄H₅BClF₈N₆) [M + H]⁺, 575.0230; found, 575.0220; UV-vis (THF): λ_{max} (nm) (log ε (M^{−1}·cm^{−1})), 298 nm (4.6), 576 nm (4.7).

SPc(AB₂)—*Boron 1,2,3,4-tetrafluorophthalocyanine chloride*. The synthesis was completed using an analogous procedure with the following proportions of reagents: phthalonitrile (0.273 g, 2.13 mmol), tetrafluorophthalonitrile (0.141 g, 0.704 mmol), *p*-xylene (10 mL), BCl₃ (1 M in *p*-xylene, 1.5 mL, 1.5 mmol). A dark purple solid was obtained (0.031 g, 9%). ¹H NMR (400 MHz, CDCl₃) δ (ppm): 8.00–8.04 (m, 4H), 8.90–8.94 (m, 4H); ¹⁹F NMR (376 MHz, CDCl₃) δ (ppm): −140.3 (d, *J* = 16 Hz, 2F), −151.7 (d, *J* = 16 Hz, 2F); HR-LCMS APCI: calcd. for (C₂₄H₉BClF₄N₆) [M + H]⁺, 503.0606; found, 503.0606; UV-vis (THF): λ_{max} (nm) (log ε (M^{−1}·cm^{−1})), 306 nm (4.5), 572 nm (4.7).

SPc(A₃)—*Boron 1,2,3,4,8,9,10,11,15,16,17,18-dodecafluorophthalocyanine chloride*. 6 g scale, 17% yield; ¹⁹F NMR (376 MHz, CDCl₃) δ (ppm): −136.7 (d, *J* = 17 Hz, 8F), −147.4 (d, *J* = 17 Hz, 8F).

SPc(A₂C)—*Boron 1,2,3,4,8,9,10,11-octafluoro-naphtho[b] subphthalocyanine chloride*. 2 g scale, 2% yield; ¹⁹F NMR (376 MHz, CDCl₃) δ (ppm): −138.8 (m, 2F), −138.9 (m, 2F), −149.2 (m, 2F), −150.6 (m, 2F)

SPc(AC₂)—*Boron 1,2,3,4-tetrafluoro-dinaphtho[b,g] subphthalocyanine chloride*. 2 g scale, 3% yield; ¹⁹F NMR (376 MHz, CDCl₃) δ (ppm): −141.8 (d, 17 Hz, 2F), −153.7 (d, 17 Hz, 2F)

3.4. Fluorescence Quantum Yield Determination

Fluorescence quantum yields were determined by the relative method [31], using cresyl violet (Φ_f = 0.54, methanol) as a standard [32], and analysis with Equation (1) where *r* and *x* denote the standard and unknown, respectively, *A* is the absorption intensity at the excitation wavelength, *F* is the integrated fluorescence intensity, and *n* is the refractive index of the solvent. Cross calibration determined less than 10% error for this method and instrumentation.

$$\Phi_x = \Phi_r \cdot \left(\frac{A_r \cdot F_x \cdot n_x^2}{A_x \cdot F_r \cdot n_r^2} \right) \quad (1)$$

3.5. Cell Culture and Fluorescence Imaging

Cell culture reagents were obtained from Hyclone (GE) unless otherwise noted. MDA-MB-231 breast tumor cells were obtained from American Type Culture Collection and maintained in Dulbecco's Modified Eagle Medium (DMEM) supplemented with 10% fetal bovine serum. For imaging assays, cells were plated in 12-well plates (Corning, Corning, NY, USA) and allowed to grow to ca. 50% confluency before being treated with solutions of SPcs in media (0.2% dimethylsulfoxide). Images were collected with a VWR Inverted Fluorescence Microscope, Moticam 5.0 (Motic, Hong Kong) and TRITC filter set (λ_{ex} = 540 nm ± 12 nm, λ_{em} = 605 nm ± 27 nm).

4. Conclusions

We have reported here the synthesis of novel mixed fluorinated SPcs and provided a comparison to a number of known analogs of similar structure. Of particular note is the tabulation of the effects of

step-wise synthetic modification on physical properties relevant to the development of NIR fluorescent probes based on this SPc platform. Fluorinated SPcs have been shown to be taken up by MDA-MB-231 breast tumor cells where significant intracellular fluorescence is observed. Future directions include further study into synthetic methods to bathochromically shift emission and improve solubility for ultimate application of this family of molecules as NIR fluorescent imaging probes.

Supplementary Materials: Supplementary materials can be found at www.mdpi.com/1422-0067/18/6/1177/s1.

Acknowledgments: The authors would like to acknowledge generous funding from the Michigan Space Grant Consortium (Research Seed Grant, Evan R. Trivedi; Undergraduate Research Fellowship, Megan A. Kaster), the Oakland University Research Committee (Faculty Fellowship, Evan R. Trivedi), the Oakland University Office of the Provost & Vice President for Academic Affairs (Provost Undergraduate Research Award, Katherine J. McAuliffe), Chrysler L.L.C. (Chrysler Undergraduate Student Research Award, Megan A. Kaster), and Mark Dershwitz (Dershwitz Summer Research Award, Megan A. Kaster and Katherine J. McAuliffe).

Author Contributions: Evan R. Trivedi conceived and designed the experiments and wrote the manuscript. Katherine J. McAuliffe, Megan A. Kaster, and Regina G. Szlag performed the experiments and analyzed the data.

Conflicts of Interest: The authors declare no conflict of interest.

Abbreviations

SPc	Subphthalocyanine
Pc	Phthalocyanine
NIR	Near-infrared
LUMO	Lowest unoccupied molecular orbital
THF	Tetrahydrofuran
HPLC	High performance liquid chromatography
DMSO	Dimethylsulfoxide
DMEM	Dulbecco's modified eagle medium

References

1. Meller, A.; Ossko, A. Phthalocyaninartige bor-komplexe. *Monatsh. Für Chem.* **1972**, *103*, 150. [[CrossRef](#)]
2. Claessens, C.G.; Gonzalez-Rodriguez, D.; Rodriguez-Morgade, M.S.; Medina, A.; Torres, T. Subphthalocyanines, subporphyrines, and subporphyrins: Singular nonplanar aromatic systems. *Chem. Rev.* **2014**, *114*, 2192–2277. [[CrossRef](#)] [[PubMed](#)]
3. Shimizu, S.; Kobayashi, N. Structurally-modified subphthalocyanines: Molecular design towards realization of expected properties from the electronic structure and structural features of subphthalocyanine. *Chem. Commun.* **2014**, *50*, 6949–6966. [[CrossRef](#)] [[PubMed](#)]
4. Fulford, M.V.; Jaidka, D.; Paton, A.S.; Morse, G.E.; Brisson, E.R.L.; Lough, A.J.; Bender, T.P. Crystal structures, reaction rates, and selected physical properties of halo-boronsubphthalocyanines (halo = fluoride, chloride, and bromide). *J. Chem. Eng. Data* **2012**, *57*, 2756–2765. [[CrossRef](#)]
5. Claessens, C.G.; Torres, T. Subphthalocyanine enantiomers: First resolution of a C3 aromatic compound by HPLC. *Tetrahedron Lett.* **2000**, *41*, 6361–6365. [[CrossRef](#)]
6. Zyskowski, C.D.; Kennedy, V.O. Compounds in the series from boron subphthalocyanine to boron subnaphthalocyanine. *J. Porphy. Phthalocyanines* **2000**, *4*, 707–712. [[CrossRef](#)]
7. Stork, J.R.; Potucek, R.J.; Durfee, W.S.; Noll, B.C. The synthesis and structure of mixed subphthalocyanine/subnaphthalocyanine complexes. *Tetrahedron Lett.* **1999**, *40*, 8055–8058. [[CrossRef](#)]
8. Shimizu, S.; Nakano, S.; Hosoya, T.; Kobayashi, N. Pyrene-fused subphthalocyanine. *Chem. Commun.* **2011**, *47*, 316–318. [[CrossRef](#)] [[PubMed](#)]
9. Shimizu, S.; Nakano, S.; Kojima, A.; Kobayashi, N. A core-expanded subphthalocyanine analogue with a significantly distorted conjugated surface and unprecedented properties. *Angew. Chem. Int. Ed.* **2014**, *53*, 2408–2412. [[CrossRef](#)] [[PubMed](#)]
10. Zhang, R.R.; Schroeder, A.B.; Grudzinski, J.J.; Rosenthal, E.L.; Warram, J.M.; Pinchuk, A.N.; Eliceiri, K.W.; Kuo, J.S.; Weichert, J.P. Beyond the margins: Real-time detection of cancer using targeted fluorophores. *Nat. Rev. Clin. Oncol.* **2017**, *14*, 347–364. [[CrossRef](#)] [[PubMed](#)]

11. Adams, K.E.; Ke, S.; Kwon, S.; Liang, F.; Fan, Z.; Lu, Y.; Hirschi, K.; Mawad, M.E.; Barry, M.A.; Sevick-Muraca, E.M. Comparison of visible and near-infrared wavelength-excitable fluorescent dyes for molecular imaging of cancer. *J. Biomed. Opt.* **2007**, *12*, 024017. [[CrossRef](#)] [[PubMed](#)]
12. Sevick-Muraca, E.M. Translation of near-infrared fluorescence imaging technologies: Emerging clinical applications. *Annu. Rev. Med.* **2012**, *63*, 217–231. [[CrossRef](#)] [[PubMed](#)]
13. Quaresima, V.; Matcher, S.J.; Ferrari, M. Identification and quantification of intrinsic optical contrast for near-infrared mammography. *Photochem. Photobiol.* **1998**, *67*, 4–14. [[CrossRef](#)] [[PubMed](#)]
14. Van Driel, P.; van der Vorst, J.R.; Verbeek, F.P.R.; Oliveira, S.; Snoeks, T.J.A.; Keereweer, S.; Chan, B.; Boonstra, M.C.; Frangioni, J.V.; van Bergen en Henegouwen, P.M.P.; et al. Intraoperative fluorescence delineation of head and neck cancer with a fluorescent anti-epidermal growth factor receptor nanobody. *Int. J. Cancer* **2014**, *134*, 2663–2673. [[CrossRef](#)] [[PubMed](#)]
15. Tummers, Q.R.J.G.; Verbeek, F.P.R.; Schaafsma, B.E.; Boonstra, M.C.; van der Vorst, J.R.; Liefers, G.J.; van de Velde, C.J.H.; Frangioni, J.V.; Vahrmeijer, A.L. Real-time intraoperative detection of breast cancer using near-infrared fluorescence imaging and methylene blue. *Eur. J. Surg. Oncol.* **2014**, *40*, 850–858. [[CrossRef](#)] [[PubMed](#)]
16. Ishii, K.; Kobayashi, N. 102—The photophysical properties of phthalocyanines and related compounds. In *The Porphyrin Handbook*; Smith, K.M., Guillard, R., Eds.; Academic Press: Amsterdam, The Netherlands, 2003; pp. 1–42.
17. Lobo, A.C.S.; Silva, A.D.; Tomé, V.A.; Pinto, S.M.A.; Silva, E.F.F.; Calvete, M.J.F.; Gomes, C.M.F.; Pereira, M.M.; Arnaut, L.G. Phthalocyanine labels for near-infrared fluorescence imaging of solid tumors. *J. Med. Chem.* **2016**, *59*, 4688–4696. [[CrossRef](#)] [[PubMed](#)]
18. Avşar, G.; Sari, F.A.; Yuzer, A.C.; Soylu, H.M.; Er, O.; Ince, M.; Lambrecht, F.Y. Intracellular uptake and fluorescence imaging potential in tumor cell of zinc phthalocyanine. *Int. J. Pharm.* **2016**, *505*, 369–375. [[CrossRef](#)] [[PubMed](#)]
19. Lv, F.; He, X.; Wu, L.; Liu, T. Lactose substituted zinc phthalocyanine: A near infrared fluorescence imaging probe for liver cancer targeting. *Bioorg. Med. Chem. Lett.* **2013**, *23*, 1878–1882. [[CrossRef](#)] [[PubMed](#)]
20. Trivedi, E.R.; Harney, A.S.; Olive, M.B.; Podgorski, I.; Moin, K.; Sloane, B.F.; Barrett, A.G.M.; Meade, T.J.; Hoffman, B.M. Chiral porphyrazine near-IR optical imaging agent exhibiting preferential tumor accumulation. *Proc. Natl. Acad. Sci. USA* **2010**, *107*, 1284–1288. [[CrossRef](#)] [[PubMed](#)]
21. Xu, H.; Jiang, X.J.; Chan, E.Y.M.; Fong, W.P.; Ng, D.K.P. Synthesis, photophysical properties and in vitro photodynamic activity of axially substituted subphthalocyanines. *Org. Biomol. Chem.* **2007**, *5*, 3987–3992. [[CrossRef](#)] [[PubMed](#)]
22. Bernhard, Y.; Winckler, P.; Chassagnon, R.; Richard, P.; Gigot, E.; Perrier-Cornet, J.M.; Decreau, R.A. Subphthalocyanines: Addressing water-solubility, nano-encapsulation, and activation for optical imaging of B16 melanoma cells. *Chem. Commun.* **2014**, *50*, 13975–13978. [[CrossRef](#)] [[PubMed](#)]
23. Farley, C.; Bhupathiraju, N.V.S.D.K.; John, B.K.; Drain, C.M. Tuning the structure and photophysics of a fluororous phthalocyanine platform. *J. Phys. Chem. A* **2016**, *120*, 7451–7464. [[CrossRef](#)] [[PubMed](#)]
24. Garcia, A.M.; Alarcon, E.; Munoz, M.; Scaiano, J.C.; Edwards, A.M.; Lissi, E. Photophysical behaviour and photodynamic activity of zinc phthalocyanines associated to liposomes. *Photochem. Photobiol. Sci.* **2011**, *10*, 507–514. [[CrossRef](#)] [[PubMed](#)]
25. Filler, R.; Saha, R. Fluorine in medicinal chemistry: A century of progress and a 60-year retrospective of selected highlights. *Future Med. Chem.* **2009**, *1*, 777–791. [[CrossRef](#)] [[PubMed](#)]
26. Biffinger, J.C.; Kim, H.W.; DiMagno, S.G. The polar hydrophobicity of fluorinated compounds. *Chembiochem* **2004**, *5*, 622–627. [[CrossRef](#)] [[PubMed](#)]
27. Claessens, C.G.; Gonzalez-Rodriguez, D.; del Rey, B.; Torres, T.; Mark, G.; Schuchmann, H.-P.; von Sonntag, C.; MacDonald, J.G.; Nohr, R.S. Highly efficient synthesis of chloro- and phenoxy-substituted subphthalocyanines. *Eur. J. Org. Chem.* **2003**, 2547–2551. [[CrossRef](#)]
28. Fifolt, M.J.; Sojka, S.A.; Wolfe, R.A.; Hojnicky, D.S.; Bieron, J.F.; Dinan, F.J. A chemical shift additivity method for the prediction of fluorine-19 chemical shifts in fluoroaromatic compounds. *J. Org. Chem.* **1989**, *54*, 3019–3023. [[CrossRef](#)]
29. Gouterman, M.; Snyder, L.C.; Wagniere, G.H. Spectra of porphyrins: Part II. Four orbital model. *J. Mol. Spectrosc.* **1963**, *11*, 108–127. [[CrossRef](#)]

30. Wheeler, B.L.; Nagasubramanian, G.; Bard, A.J.; Schechtman, L.A.; Kenney, M.E. A silicon phthalocyanine and a silicon naphthalocyanine: Synthesis, electrochemistry, and electrogenerated chemiluminescence. *J. Am. Chem. Soc.* **1984**, *106*, 7404–7410. [[CrossRef](#)]
31. Williams, A.T.R.; Winfield, S.A.; Miller, J.N. Relative fluorescence quantum yields using a computer-controlled luminescence spectrometer. *Analyst* **1983**, *108*, 1067–1071. [[CrossRef](#)]
32. Magde, D.; Brannon, J.H.; Cremers, T.L.; Olmsted, J. Absolute luminescence yield of cresyl violet. A standard for the red. *J. Phys. Chem.* **1979**, *83*, 696–699. [[CrossRef](#)]



© 2017 by the authors. Licensee MDPI, Basel, Switzerland. This article is an open access article distributed under the terms and conditions of the Creative Commons Attribution (CC BY) license (<http://creativecommons.org/licenses/by/4.0/>).